

# Phonon-particle coupling effects in single-particle energies of semi-magic nuclei.

E. E. Saperstein<sup>\*,\*\*1)</sup>, M. Baldo<sup>†</sup>, S. S. Pankratov<sup>\*,\*\*\*</sup>, S. V. Tolokonnikov<sup>\*,\*\*\*</sup>

<sup>\*</sup>National Research Centre Kurchatov Institute, pl. Akademika Kurchatova 1, Moscow, 123182 Russia

<sup>\*\*</sup>National Research Nuclear University MEPhI, 115409 Moscow, Russia

<sup>†</sup>INFN, Sezione di Catania, 64 Via S.-Sofia, I-95125 Catania, Italy

<sup>\*\*\*</sup>Moscow Institute of Physics and Technology, 141700 Dolgoprudny, Russia

Submitted June 17, 2019

A method is presented to evaluate the particle-phonon coupling (PC) corrections to the single-particle energies (SPEs) in semi-magic nuclei. In such nuclei always there is a collective low-lying  $2^+$  phonon, and a strong mixture of single-particle and particle-phonon states often occurs. As in magic nuclei, the so-called  $g_L^2$  approximation, where  $g_L$  is the vertex of the  $L$ -phonon creation, can be used for finding the PC correction  $\delta\Sigma^{\text{PC}}(\varepsilon)$  to the initial mass operator  $\Sigma_0$ . In addition to the usual pole diagram, the phonon “tadpole” diagram is also taken into account. In semi-magic nuclei, the perturbation theory in  $\delta\Sigma^{\text{PC}}(\varepsilon)$  with respect to  $\Sigma_0$  is often invalid for finding the PC corrected SPEs. Instead, the Dyson equation with the mass operator  $\Sigma(\varepsilon)=\Sigma_0+\delta\Sigma^{\text{PC}}(\varepsilon)$  is solved directly, without any use of the perturbation theory. Results for a chain of semi-magic Pb isotopes are presented.

PACS: 21.60.-n; 21.65.+f; 26.60.+c; 97.60.Jd

Last decade, there was a revival of the interest within different self-consistent nuclear approaches to study the particle-phonon coupling (PC) effects in the single-particle energies (SPEs) of magic nuclei. We cite here such studies within the relativistic mean-field theory [1], within the Skyrme–Hartree–Fock method [2, 3, 4] and on the basis of the self-consistent theory of finite Fermi systems (TFFS) [5]. The Fayans energy density functional (EDF) was used in the last case to find the self-consistent basis. In all the references cited above double-magic nuclei were considered. There are several reasons for such choice. First, these nuclei are non-superfluid which simplifies the theoretical analysis. Second, the so-called  $g_L^2$  approximation is, as a rule, valid in magic nuclei,  $g_L$  being the vertex of the  $L$ -phonon creation. Moreover, the perturbation theory in terms of the PC correction to the mass operator is also applicable, which makes evaluation of PC corrected SPEs rather simple. At last, there is a lot of experimental data on SPEs in these nuclei [6].

In this work, we extend the field of this problem to semi-magic nuclei. Unfortunately, the experimental data on the SPEs in semi-magic nuclei are rather scarce. Indeed, the single-particle spectroscopic factor  $S$  of an excited state under consideration should be known. In addition, its value should be rather large, in order that one can interpret this state as a single-particle one. Extraction of the spectroscopic factors from the reaction

data is a complicated theoretical problem, therefore the list of known spectroscopic factors is rather limited. However, the PC corrections to the SPEs are necessary not only by themselves, they are also usually important ingredients of the procedure of finding PC corrections to other nuclear characteristics, e.g., magnetic moments and  $M1$  transitions in odd nuclei [7, 8, 9]. PC corrections to the double odd-even mass differences found in the approach starting from the free  $NN$  potential [10, 11] is another example where the PC corrections to SPEs are of primary importance.

A semi-magic nucleus consists of two sub-systems with different properties. One of them, magic, is normal, whereas the non-magic counterpart is superfluid. We will consider the SPEs of the normal sub-system only. Therefore, the main part of the formalism for description of the PC corrections developed for magic nuclei [5] remains valid. One difference with double-magic nuclei is that the vertex  $g_L(\mathbf{r})$  obeys the QRPA-like TFFS equation in superfluid nuclei, in contrast to simple RPA-like equation in magic nuclei. This complication is not very serious as we developed the necessary method with the use of the Fayans EDF in a previous paper [12]. A real difficulty arises in non-magic nuclei due to appearance of low-lying  $2^+$  states which is a characteristic feature of such nuclei. As a result, small denominators appear regularly in the expressions for the PC corrections which makes unapplicable a plane perturbation theory.

<sup>1)</sup>e-mail: Sapershtein\_EE@nrcki.ru

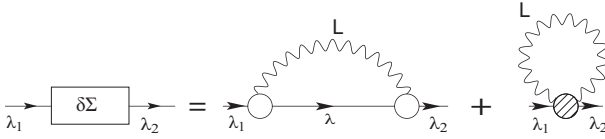


Fig. 1. PC corrections to the mass operator. The gray blob denotes the phonon “tadpole” term.

To find the SPEs with account for the PC effects, we solve the following equation:

$$(\varepsilon - H_0 - \delta\Sigma^{\text{PC}}(\varepsilon)) \phi = 0, \quad (1)$$

where  $H_0$  is the quasiparticle Hamiltonian with the spectrum  $\varepsilon_\lambda^{(0)}$  and  $\delta\Sigma^{\text{PC}}$  is the PC correction to the quasiparticle mass operator. This is equivalent to the Dyson equation for the one-particle Green function  $G$  with the mass operator  $\Sigma = \Sigma_0 + \delta\Sigma^{\text{PC}}(\varepsilon)$ .

In magic nuclei [5, 10, 11] the perturbation theory in  $\delta\Sigma^{\text{PC}}$  with respect to  $H_0$  was used to solve this equation:

$$\varepsilon_\lambda = \varepsilon_\lambda^{(0)} + Z_\lambda^{\text{PC}} \delta\Sigma_{\lambda\lambda}^{\text{PC}}(\varepsilon_\lambda^{(0)}), \quad (2)$$

where

$$Z_\lambda^{\text{PC}} = \left( 1 - \left( \frac{\partial}{\partial \varepsilon} \delta\Sigma^{\text{PC}}(\varepsilon) \right)_{\varepsilon=\varepsilon_\lambda^{(0)}} \right)^{-1}. \quad (3)$$

In this article, we will solve Eq. (1) directly, without any additional approximations. As to the  $g_L^2$ -approximation for the PC correction  $\delta\Sigma^{\text{PC}}$  to the mass operator, it remains valid in semi-magic nuclei, and only the next step from (1) to (2) becomes invalid. In the case when several  $L$ -phonons are taken into account, the total PC variation of the mass operator in Eqs. (1)–(3) is just the sum:

$$\delta\Sigma^{\text{PC}} = \sum_L \delta\Sigma_L^{\text{PC}}. \quad (4)$$

The diagrams for the  $\delta\Sigma_L^{\text{PC}}$  operator within the  $g_L^2$ -approximation are displayed in Fig. 1. The first one is the usual pole diagram, with obvious notation, whereas the second, “tadpole” diagram represents the sum of all non-pole diagrams of order  $g_L^2$ .

Explicit expression for the pole term is well known [1, 5, 10], and we present it just for completeness:

$$\delta\Sigma_{\lambda\lambda}^{\text{pole}}(\varepsilon) = \sum_{\lambda_1 M} |\langle \lambda_1 | g_{LM} | \lambda \rangle|^2 \times \left( \frac{n_{\lambda_1}}{\varepsilon + \omega_L - \varepsilon_{\lambda_1}^{(0)}} + \frac{1 - n_{\lambda_1}}{\varepsilon - \omega_L - \varepsilon_{\lambda_1}^{(0)}} \right), \quad (5)$$

where  $\omega_L$  is the excitation energy of the  $L$ -phonon and  $n_\lambda = (1, 0)$  are the particle occupation number (remind

that we deal with the normal subsystem of a semi-magic nucleus).

The vertex  $g_L(\mathbf{r})$  obeys the QRPA-like TFFS equation [13],

$$\hat{g}_L(\omega) = \hat{\mathcal{F}} \hat{A}(\omega) \hat{g}_L(\omega), \quad (6)$$

where all the terms are matrices. In the standard TFFS notation, we have:

$$\hat{g}_L = \begin{pmatrix} g_L^{(0)} \\ g_L^{(1)} \\ g_L^{(2)} \end{pmatrix}, \quad (7)$$

$$\hat{\mathcal{F}} = \begin{pmatrix} \mathcal{F} & \mathcal{F}^{\omega\xi} & \mathcal{F}^{\omega\xi} \\ \mathcal{F}^{\xi\omega} & \mathcal{F}^\xi & \mathcal{F}^{\xi\omega} \\ \mathcal{F}^{\xi\omega} & \mathcal{F}^{\xi\omega} & \mathcal{F}^\xi \end{pmatrix}. \quad (8)$$

In (7),  $g^{(0)}$  is the normal component of the vertex  $\hat{g}$ , whereas  $g^{(1),(2)}$  are two anomalous ones. In Eq. (8),  $\mathcal{F}$  is the usual Landau–Migdal interaction amplitude which is the second variation derivative of the EDF  $\mathcal{E}[\rho, \nu]$  over the normal density  $\rho$ . The effective pairing interaction  $\mathcal{F}^\xi$  is the second derivative of the EDF over the anomalous density  $\nu$ . At last, the amplitude  $\mathcal{F}^{\xi\omega}$  stands for the mixed derivative of  $\mathcal{E}$  over  $\rho$  and  $\nu$ .

The matrix  $\hat{A}$  consists of  $3 \times 3$  integrals over  $\varepsilon$  of the products of different combinations of the Green function  $G(\varepsilon)$  and two Gor’kov functions  $F^{(1)}(\varepsilon)$  and  $F^{(2)}(\varepsilon)$  [13].

As we need the proton vertex  $\hat{g}_L^p$  and the proton subsystem is normal, only the normal vertex  $g_L^{(0)p}$  is non-zero in this case. This is explicit meaning of the short notation  $g_L$  in (5) and below.

For solving the above equations, we use the self-consistent basis generated by the version DF3-a [14] of the Fayans EDF [15, 16]. The nuclear mean-field potential  $U(r)$  is the first derivative of  $\mathcal{E}$  over  $\rho$ .

All low-lying phonons we deal with are of surface nature, the surface peak dominating in their creation amplitude:

$$g_L(r) = \alpha_L \frac{dU}{dr} + \chi_L(r). \quad (9)$$

The first term in this expression is surface peaked, whereas the in-volume term  $\chi_L(r)$  is rather small. It is illustrated in Fig. 2 for the  $2_1^+$  and  $3_1^-$  states in  $^{204}\text{Pb}$ . In this work, just as in [5, 10, 11], we neglect the in-volume term in (9) when considering the tadpole PC term of  $\delta\Sigma_L^{\text{PC}}$ . In the result, it is reduced [5] to rather simple form:

$$\delta\Sigma_L^{\text{tad}} = \frac{\alpha_L^2}{2} \frac{2L+1}{3} \Delta U(r). \quad (10)$$

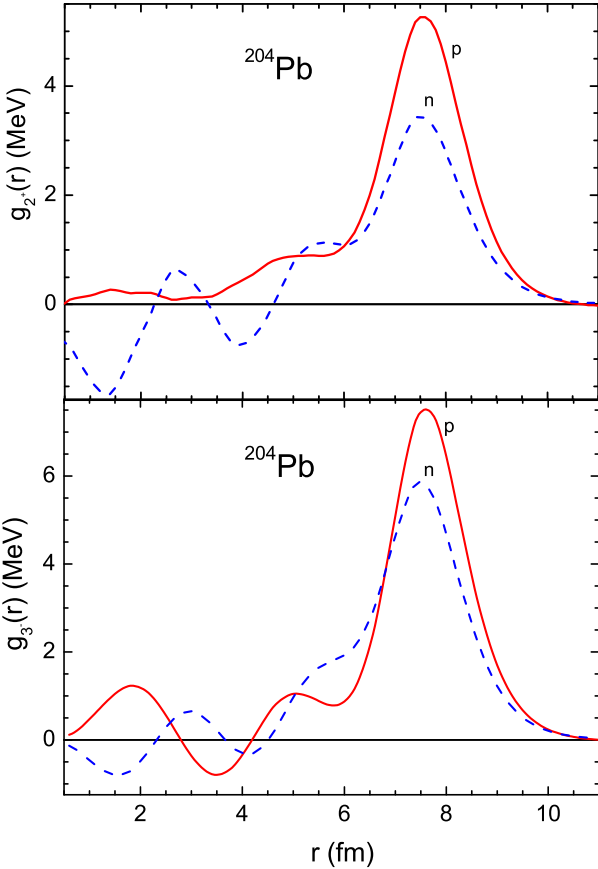


Fig2. (Color online) Phonon creation amplitudes  $g_L(r)$  for two low-lying phonons in  $^{204}\text{Pb}$ .

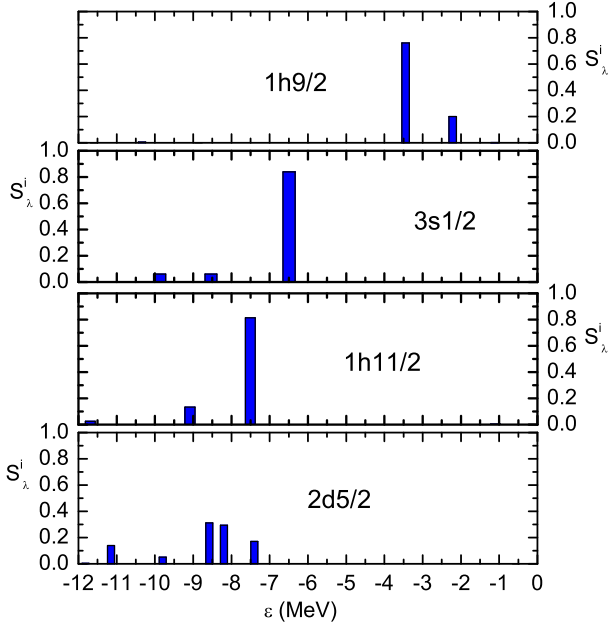


Fig3. (Color online)  $Z$ -factors.

Note that the above scheme for the ghost ( $L=1$ ,  $\omega_1=0$ ) phonon results in an explicit expression for the “recoil effect.” Details can be found in [5].

In this work, we limit ourselves with four even lead isotopes,  $^{200,202,204,206}\text{Pb}$ . In all cases we consider two low-lying phonons,  $2_1^+$  and  $3_1^-$ . Their excitation energies are presented in Table 1. As one can see, they agree with existing experimental data sufficiently well. The ghost  $1^-$  is also taken into account, although the corresponding correction for nuclei under consideration is very small, because it depends on the mass number as  $1/A$ .

Table 1. Excitation energies  $\omega_{2,3}$  (MeV) of the  $2_1^+$  and  $3_1^-$  phonons in even Pb isotopes.

nucleus	$\omega_2^{\text{th}}$	$\omega_2^{\text{exp}}$	$\omega_3^{\text{th}}$	$\omega_3^{\text{exp}}$
$^{200}\text{Pb}$	0.789	1.026	2.620	-
$^{202}\text{Pb}$	0.823	0.960	2.704	2.517
$^{204}\text{Pb}$	0.882	0.899	2.785	2.621
$^{206}\text{Pb}$	0.945	0.803	2.839	2.648

Let us go to the description of the method we use to solve Eq. (1). As the PC corrections are important only for the SPEs nearby the Fermi surface, we limit ourselves with a model space  $S_0$  including two shells close to it, i.e. one hole and one particle shells, and besides we retain only the negative energy states. To avoid any misunderstanding, we stress that this restriction concerns only Eq. (1). In Eq. (5) for  $\delta\Sigma^{\text{pole}}$ , we use rather wide single-particle space with energies  $\varepsilon_\lambda^{(0)} < 40$  MeV. We take as an example to illustrate the method the nucleus  $^{204}\text{Pb}$  which is sufficiently distant from the double-magic  $^{208}\text{Pb}$  to be considered as a typical semi-magic. The space  $S_0$  involves 5 hole states ( $1g_{7/2}$ ,  $2d_{5/2}$ ,  $1h_{11/2}$ ,  $2d_{3/2}$ ,  $3s_{1/2}$ ) and four particle ones ( $1g_{9/2}$ ,  $2f_{7/2}$ ,  $1i_{13/2}$ ,  $2f_{5/2}$ ). We see that there is here only one state for each  $(l, j)$  value. Therefore, we need only diagonal elements  $\delta\Sigma_{\lambda\lambda}^{\text{pole}}$  (5), which simplifies very much the solution of the Dyson equation. In the result, Eq. (1) reduces as follows:

$$\varepsilon - \varepsilon_\lambda^{(0)} - \delta\Sigma_{\lambda\lambda}^{\text{PC}}(\varepsilon) = 0, \quad (11)$$

The tadpole term does not depend on the energy, therefore only poles of Eq. (5) are the singular points of Eq. (11). They can be readily found from (5) in terms of  $\varepsilon_\lambda^{(0)}$  and  $\omega_L$ . It can be easily seen that the lhs of Eq. (11) always changes sign between any couple of neighboring poles, and the corresponding solution  $\varepsilon_\lambda^i$  can be found with usual methods. In this notation,  $\lambda$  is just the index for the initial single-particle state from which

the state  $|\lambda, i\rangle$  originated. The latter is a mixture of a single-particle state with several particle-phonon states. The corresponding single-particle strength distribution factors ( $S$ -factors) can be found similar to (3):

$$S_\lambda^i = \left( 1 - \left( \frac{\partial}{\partial \varepsilon} \delta \Sigma^{\text{PC}}(\varepsilon) \right)_{\varepsilon=\varepsilon_\lambda^i} \right)^{-1}. \quad (12)$$

Evidently, they should obey the normalization rule:

$$\sum_i S_\lambda^i = 1. \quad (13)$$

Accuracy of fulfillment of this relation is a measure of validity of the model space  $S_0$  we use to solve the problem under consideration. In the major part of the cases we will consider it is fulfilled with 1–2% accuracy.

A set of solutions for four  $|\lambda, i\rangle$  states in  $^{204}\text{Pb}$  is presented in Table 2. The corresponding  $S$ -factors are displayed in Fig. 3. In three upper cases for a given  $\lambda$  there is a state  $|\lambda, i_0\rangle$  with dominating  $S_\lambda^{i_0}$  value ( $\simeq 0.8$ ). They are examples of “good” single-particle states. In such cases, the following prescription looks natural for the PC corrected single-particle characteristics:

$$\varepsilon_\lambda = \varepsilon_\lambda^{i_0}; \quad Z_\lambda^{\text{PC}} = S_\lambda^{i_0}. \quad (14)$$

This is an analog of Eqs. (2) and (3) in the perturbative solution.

The lowest panel in Fig. 3 represents a case of a strong spread where there are two or more numbers  $i$  with comparable values of the spectroscopic factors  $S_\lambda^i$ . In such cases, we suggest the following generalization of Eq. (14):

$$\varepsilon_\lambda = \frac{1}{Z_\lambda^{\text{PC}}} \sum_i \varepsilon_\lambda^i S_\lambda^i, \quad (15)$$

where

$$Z_\lambda^{\text{PC}} = \sum_i S_\lambda^i. \quad (16)$$

In both the above sums, only the states  $|\lambda, i\rangle$  with appreciable values of  $S_\lambda^i$  are included. In practice, we include in these sums the states with  $S_\lambda^i > 0.1$ . The value of  $\varepsilon_\lambda$  is just the centroid of the single particle energy distribution.

The results for SPEs and  $Z$ -factors are presented in Table 3. For each segment of the table which relates to the even core  $^A\text{Pb}$ , the lower part, till the  $3s_{1/2}$  state, describes the proton holes, i. e. the states of the  $^{A-1}\text{Tl}$  nucleus. On the contrary, the upper states are the proton particle states, i.e. they belong to the  $^{A+1}\text{Bi}$  nucleus. The tadpole term is given separately. The recoil correction is not presented explicitly as it is very small in the lead region, the maximum value is  $\delta\varepsilon_\lambda(1^-) = 0.04$

Table 2. Examples of solutions of Eq. (11) for protons in  $^{204}\text{Pb}$ .

$\lambda$	$i$	$\varepsilon_\lambda^i$	$S_\lambda^i$
$2d_{5/2}$	1	-11.817	$0.314 \times 10^{-2}$
	2	-11.150	0.139
	3	-9.799	$0.516 \times 10^{-1}$
	4	-8.580	0.312
	5	-8.195	0.295
	6	-7.404	0.171
	7	-0.564	$0.791 \times 10^{-3}$
$1h_{11/2}$	1	-13.717	$0.692 \times 10^{-3}$
	2	-11.690	$0.256 \times 10^{-1}$
	3	-9.084	0.134
	4	-7.509	0.814
	5	-2.471	$0.427 \times 10^{-3}$
	6	-1.095	$0.473 \times 10^{-2}$
$3s_{1/2}$	1	-9.877	$0.608 \times 10^{-1}$
	2	-8.536	$0.604 \times 10^{-1}$
	3	-6.493	0.839
$1h_{9/2}$	1	-13.736	$0.220 \times 10^{-2}$
	2	-11.596	$0.777 \times 10^{-3}$
	3	-10.339	$0.674 \times 10^{-2}$
	4	-8.862	$0.484 \times 10^{-3}$
	5	-3.447	0.760
	6	-2.217	0.199
	7	-1.122	$0.288 \times 10^{-2}$

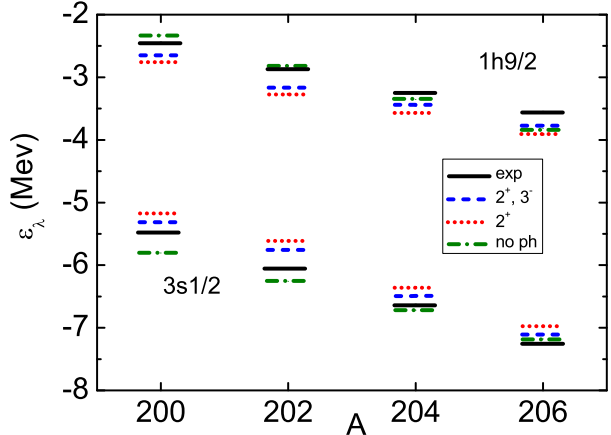


Fig4. (Color online) SPEs corresponding to the ground states of the odd Tl and Bi isotopes, the proton-odd neighbors of the  $^4\text{Pb}$  nucleus, the  $3s_{1/2}$  and  $1h_{9/2}$  states correspondingly, with and without PC corrections.

Table 3. PC corrected proton single-particle characteristics of even Pb isotopes.

nucleus	$\lambda$	$\varepsilon_\lambda^0$	$\delta\varepsilon_\lambda^{\text{tad}}$	$\varepsilon_\lambda$	$Z_\lambda$
$^{200}\text{Pb}$	$1i_{13/2}$	-0.26	0.39	-0.13	0.96
	$2f_{7/2}$	-1.05	0.24	-1.35	0.83
	$1g_{9/2}$	-2.33	0.33	-2.21	0.93
	$3s_{1/2}$	-5.81	0.20	-5.80	0.89
	$2d_{3/2}$	-6.67	0.21	-6.50	0.89
	$1h_{11/2}$	-7.06	0.37	-6.81	0.93
	$2d_{5/2}$	-7.88	0.21	-7.60	0.88
	$1g_{7/2}$	-9.97	0.29	-9.89	0.91
$^{202}\text{Pb}$	$1i_{13/2}$	-0.74	0.41	-0.61	0.95
	$2f_{7/2}$	-1.52	0.25	-1.81	0.83
	$1g_{9/2}$	-2.86	0.34	-2.73	0.93
	$3s_{1/2}$	-6.26	0.21	-6.25	0.89
	$2d_{3/2}$	-7.09	0.22	-6.92	0.89
	$1h_{11/2}$	-7.52	0.38	-7.27	0.93
	$2d_{5/2}$	-8.34	0.22	-8.04	0.87
	$1g_{7/2}$	-10.46	0.30	10.38	0.91
$^{204}\text{Pb}$	$1i_{13/2}$	-1.21	0.32	-1.07	0.97
	$2f_{7/2}$	-2.01	0.20	-2.24	0.87
	$1g_{9/2}$	-3.36	0.27	-3.19	0.96
	$3s_{1/2}$	-6.72	0.17	-6.49	0.84
	$2d_{3/2}$	-7.51	0.17	-7.46	0.94
	$1h_{11/2}$	-7.98	0.30	-7.73	0.95
	$2d_{5/2}$	-8.80	0.18	-8.63	0.92
	$1g_{7/2}$	-10.93	0.24	-10.80	0.95
$^{206}\text{Pb}$	$1i_{13/2}$	-1.67	0.30	-1.60	0.89
	$2f_{7/2}$	-2.51	0.19	-2.81	0.82
	$1g_{9/2}$	-3.82	0.25	-3.63	0.97
	$3s_{1/2}$	-7.18	0.16	-7.10	0.89
	$2d_{3/2}$	-7.91	0.16	-7.80	0.86
	$1h_{11/2}$	-8.42	0.27	-8.05	0.88
	$2d_{5/2}$	-9.28	0.16	-9.16	0.95
	$1g_{7/2}$	-11.36	0.22	-11.12	0.90

MeV. We see that the tadpole correction is comparable with the total PC correction  $\delta\varepsilon_\lambda^{\text{PC}} = \varepsilon_\lambda - \varepsilon_\lambda^0$ . What is more, the tadpole term taken into account makes, as a rule, the value of  $\delta\varepsilon_\lambda^{\text{PC}}$  smaller. Thus, for the semi-magic nuclei we see the tendency noted before in magic nuclei [5]. Namely, calculations of the PC corrections to SPEs without the tadpole term overestimate their values.

In Fig. 4, we display the SPEs corresponding to the ground states of the corresponding nuclei. In this case, the experimental values are known as they can be found in terms of mass values of neighboring odd and even nuclei [17]. Explicitly, they are equal to  $-S_p$ , the proton separation energies taken with the opposite sign. The results are compared of two sets of calculations. In the first case, the single  $2_1^+$  phonon is taken into account, whereas both the phonons,  $2_1^+$  and  $3_1^-$ , participate in the second set of calculations. We see, firstly, that the role of both phonons is comparable. Secondly, the total PC correction is rather small, and, finally, often it makes the agreement with the data worse. This is not strange as we deal with the EDF method containing phenomenological parameters fitted mainly to nuclear masses, which determine the experimental SPEs under discussion.

In general, the problem of explicit consideration of the PC corrections within the EDF method or any other self-consistent approach operating with phenomenological parameters is rather delicate. Indeed, these parameters include different PC effects implicitly. Therefore, a regular inclusion of the PC corrections inevitably should be accompanied with a readjustment of the initial parameters. In such a situation, it is a more promising method to separate the fluctuating part of the PC corrections, which changes in a non-regular way from a nucleus to another. Such a strategy was chosen, e.g., in [18] to explain an anomalous  $A$  dependence of charge radii of heavy calcium isotopes found recently by the ISOLDE collaboration [19].

A different situation occurs typically for the approaches which start from the free  $NN$  interactions. In these cases, the PC induced corrections should be just added to the main terms found with a free  $NN$  potential, and the PC correction to the SPEs is one of the necessary ingredients for such calculations. Such approach was rather popular in the last decade for the nuclear pairing problem [20, 21, 22, 23]. An analogous method was developed in [24, 25] to find the double odd-even mass differences of magic nuclei or semi-magic ones, for the normal subsystems in the last case. In this problem, a method to find the PC corrections was developed for magic nuclei in [10, 11]. In that case, a plain perturbation theory was used to find the PC corrections to the SPEs.

To resume, a method is developed to find the PC corrections to SPEs for semi-magic nuclei beyond the perturbation theory in the PC correction to the mass operator  $\delta\Sigma^{\text{PC}}(\varepsilon)$  with respect to  $\Sigma_0$ . Instead, the Dyson equation with the mass operator  $\Sigma(\varepsilon) = \Sigma_0 + \delta\Sigma^{\text{PC}}(\varepsilon)$  is solved directly, without any use of the perturbation the-

ory. The method is checked for a chain of even Pb isotopes. This makes it possible to extend to semi-magic nuclei the field of consistent consideration of the PC corrections to the double odd-even mass differences and some another problems.

We acknowledge for support the Russian Science Foundation, Grants Nos. 16-12-10155 and 16-12-10161. The work was also partly supported by the RFBR Grants 14-02-00107-a, 14-22-03040-ofi\_m and 16-02-00228-a. Calculations were partially carried out on the Computer Center of Kurchatov Institute.

1. E. Litvinova and P. Ring, Phys. Rev. C **73**, 044328 (2006).
2. Li-Gang Cao, G. Colò, H. Sagawa, and P.F. Bortignon, Phys. Rev. C **89**, 044314 (2014).
3. D. Tarpanov, J. Dobaczewski, J. Toivanen, and B.G. Carlsson, Phys. Rev. Lett. **113**, 252501 (2014).
4. M. Baldo, P.F. Bortignon, G. Colò, D. Rizzo, and L. Sci-  
acchitano, J. Phys. G: Nucl. Phys. **42**, 085109 (2015).
5. N.V. Gnezdilov, I.N. Borzov, E.E. Saperstein, and S.V. Tolokonnikov, Phys. Rev. C **89**, 034304 (2014).
6. H. Grawe, K. Langanke, and G. Martínez-Pinedo, Rep. Prog. Phys. **70**, 1525 (2007).
7. E.E. Saperstein, S. Kamerdzhev, S. Krewald, J. Speth, and S.V. Tolokonnikov, EPL, **103**, 42001 (2013).
8. E.E. Saperstein, S.P. Kamerdzhev, S. Krewald, J. Speth, and S.V. Tolokonnikov, JETP Lett **98**, 562 (2013).
9. E.E. Saperstein, O.I. Achakovskiy, S. Kamerdzhev, S. Krewald, J. Speth, and S.V. Tolokonnikov. Phys. At. Nucl. **77**, 1033 (2014).
10. E.E. Saperstein, M. Baldo, N.V. Gnezdilov, S.V. Tolokonnikov, JETP Lett., **103**, 3 (2016).
11. E.E. Saperstein, M. Baldo, N.V. Gnezdilov, S.V. Tolokonnikov, Phys. Rev. C **93**, 034302 (2016).
12. S.V. Tolokonnikov, S. Kamerdzhev, D. Voytenkov, S. Krewald, and E. E. Saperstein, Phys. Rev. C **84**, 064324 (2011).
13. A.B. Migdal *Theory of finite Fermi systems and applications to atomic nuclei* (Wiley, New York, 1967).
14. S.V. Tolokonnikov and E.E. Saperstein, Phys. At. Nucl. **73**, 1684 (2010).
15. A.V. Smirnov, S.V. Tolokonnikov, S.A. Fayans, Sov. J. Nucl. Phys. **48**, 995 (1988).
16. S.A. Fayans, S.V. Tolokonnikov, E.L. Trykov, and D. Zawischa, Nucl. Phys. A **676**, 49 (2000).
17. M. Wang, G. Audi, A.H. Wapstra, F.G. Kondev, M. MacCormick, X. Xu, and B. Pfeiffer, Chinese Physics C, **36**, 1603 (2012).
18. E.E. Saperstein, i.n. Borzov, and S.V. Tolokonnikov, JETP Lett., **104**, 216 (2016).
19. R.F. Garcia Ruiz, M.L. Bissell, K. Blaum et al. (Collaboration), Nature Physics **12**, 594 (2016).
20. F. Barranco, R.A. Broglia, G. Colo, G. Gori, E. Vigezzi, and P.F. Bortignon, Eur. Phys. J. A **21**, 57 (2004).
21. A. Pastore, F. Barranco, R.A. Broglia, and E. Vigezzi, Phys. Rev. C **78**, 024315 (2008).
22. S.S. Pankratov, M. Baldo, M.V. Zverev, U. Lombardo, E.E. Saperstein, and S.V. Tolokonnikov, JETP Lett. **90**, 612 (2009).
23. S.S. Pankratov, M.V. Zverev, M. Baldo, U. Lombardo, and E.E. Saperstein, Phys. Rev. C **84**, 014321 (2011).
24. N.V. Gnezdilov and E.E. Saperstein, JETP Lett. **95**, 603 (2012). 5.
25. E.E. Saperstein, M. Baldo, N.V. Gnezdilov, U. Lombardo, and S.S. Pankratov, EPJ Web. Conf. **38**, 05002 (2012).